Nonlinear Transmission of a Tetrabrominated Naphthalocyaninato Indium Chloride

Danilo Dini,*,† Mario J. F. Calvete,† Michael Hanack,† Richard G. S. Pong,‡ Steven R. Flom,‡ and James S. Shirk‡

Institute of Organic Chemistry, University of Tübingen, Auf der Morgenstelle 18, D-72076 Tübingen, Germany, and Optical Sciences Division, Naval Research Laboratory, Washington, D.C. 20375

Received: December 9, 2005; In Final Form: March 8, 2006

The axially substituted complex chloro indium(III) 2-tetrabromo-3-tetra-(3,5-di-*tert*-butylphenyloxy)naphthalocyanine [Br_4(*t*Bu_2PhO)$_4$NcInCl (**1**); MW = 1996] has been synthesized for the first time, and its nonlinear transmission properties have been evaluated with the *Z*-scan technique in both open and closed aperture configurations at 532 nm for nanosecond pulsed radiation. The tetrabrominated complex **1** displayed a larger positive nonlinear absorption coefficient when compared to an analogous nonbrominated naphthalocyanine [(*t*Bu_2PhO)$_8$NcInCl (**2**); MW = 2498]. The effect of the four Br atoms on the nonlinear optical behavior of **1** is evaluated, discussed, and compared with the nonlinear optical behavior of **2**. It is shown that the bromination of the naphthalocyanine ring considerably improves the limiting properties of such a system when high-intensity radiations are produced by nanosecond laser pulses at 532 nm.

Introduction

Phthalocyanines (Pcs) and naphthalocyanines (Ncs) are classes of compounds with useful photophysical properties for nonlinear transmission (NLT)[1] applications, which require strong attenuation of intense optical fields and the clear transmission of low intensity fields. Several metallophthalo-[2] and naphthalocyanines[2b,3] display an induced absorption with increasing incident light fluence in the visible spectral region. This nonlinear optical (NLO) effect has been termed reverse saturable absorption (RSA).[4] The effect takes place because pulsed radiation with high intensity (in the order of several megawatts per square centimeter), generates transient electronic excited states of Pcs and Ncs that have sufficiently long lifetime for the effective absorption of the remainder of the pulsed radiation. The occurrence of RSA implies that the absorption cross section(s) of the excited state(s), σ_{exc}, of the Pc (or Nc) is(are) greater than that of the ground state, σ_g, at the wavelength of excitation.[5]

For many practical applications of the NLT effect, it is desirable to have reverse saturable absorbers, which allow the complete transmission of light at low optical fields over a large spectral window. Many Pc-based materials have been demonstrated to fulfill these conditions in the mid-visible spectral range.[2] Expansion of the conjugated π-electron system of the Pc skeleton to form naphthalocyanines results in a red-shifted Q-band absorption and, consequently, a larger window of high optical transmission between the Q- and B-bands when compared to a Pc.[6] This red-shifted broad transmission window has inspired the synthesis of many different Nc-based structures,[2b,3d,3e,7] the excited-state properties of which have been mainly studied in the visible-NIR spectral range.

In the present work we have undertaken the synthesis of a new soluble tetrabrominated naphthalocyanine {chloro indium(III) 2-tetrabromo-3-tetra-(3,5-di-*tert*-butylphenyloxy)naphthalocyanine [Br_4(*t*Bu_2PhO)$_4$NcInCl, **1**]} (Chart 1) to evaluate the influence of bromination on the excited-state absorption properties of the resulting substituted complex. As a basis of comparison the octasubstituted complex chloro indium(III) 2,3-

CHART 1. Chloro Indium(III) Tetrabrominated Naphthalocyanine 1 (isomer with C_{4h} symmetry), and Chloro Indium(III) Octasubstituted Naphthalocyanine 2

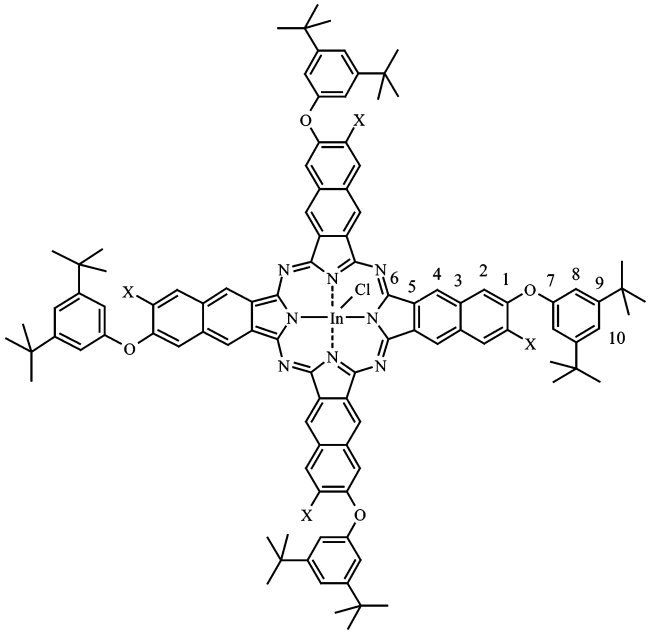

X = Br (**1**)

X = 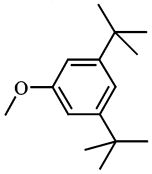 (**2**)

* To whom correspondence should be addressed. E-mail: danilo.dini@uni-tuebingen.de.

† University of Tübingen.

‡ Naval Research Laboratory.

10.1021/jp0571776 CCC: $33.50
Published on Web 06/02/2006

octa-(3,5-di-*tert*-butylphenyloxy)naphthalocyanine [$(tBu_2PhO)_8$-NcInCl, **2**] (Chart 1) was also prepared. In naphthalocyanine **1**, the presence of four di-*tert*-butylphenoxy substituents makes solubilization possible in common organic solvents even at high concentrations (on the order of 10^{-2} M), thus allowing the preparation of samples with high nonlinear optical response concomitant with relatively weak molecular aggregation.[2d] In the search for new structures with optimized NLT properties,[8] we have taken advantage of the versatility of the synthetic chemistry of Ncs, which allows the modification of the peripheral substituents, central atoms, and axial ligands in a controlled fashion with consequent production of a large number of structural variations.[9]

The peripheral halogenation of Ncs examined here is expected to bring about modifications of the electronic structure of the substituted molecule[10] due to the high electronegativity of an halogen atom. Moreover, halogenation imparts a strong polar character to the carbon−halogen bond and induces electron deficiency on the halogenated carbon atom. Such features considerably alter the redox,[11] optical,[12] electronic,[13] photophysical,[14] and photochemical[15] properties of the halogenated conjugated macrocycles by increasing their oxidation potential, lowering the HOMO level, and shifting the optical absorption to shorter wavelengths when compared to analogous unsubstituted systems.

The effects of fluorination and chlorination on the NLT effect generated by substituted Pcs and analogues have been previously examined by our group. From these studies it was concluded that fluorinated Pcs and Ncs led to an improvement of the NLT properties due to higher stability against photooxidation[3d,3e,14a] and, in case of axially substituted complexes,[16] to the increase of the transition dipole moment associated with the excited-state transition[17] producing RSA. On the other hand, analogous effects in perchlorinated Pc complexes[14b] could not be effectively evaluated since these systems formed highly aggregated species,[18] which result in excited states with relatively short lifetimes and, therefore, ineffective NLT against nanosecond pulsed radiation.[19]

The influence of bromination on the NLT effect generated by poorly soluble tetra- and octabrominated Ncs such as 2,(3)-tetrabromonaphthalocyaninato lead[20] and 2,3-octabromonaphthalocyaninato zinc[21] or octabrominated porphyrins[22] has been also studied. A conspicuous increase of the intersystem crossing (ISC, see Figure 1) rate was generally observed, which increased the yield of excited triplet state formation (tending toward unity) presumably due to the internal heavy-atom effect[23] of Br.[4c] Moreover, the presence of Br also shortened the lifetime of the excited triplet state[22b] through spin−orbit coupling[23] and the coupling between the atomic orbital of the halogen and the molecular orbital of the ligand in the excited state.[22b]

Similar results were found when the photophysical properties of iodinated porphyrins were analyzed.[22b,24] Besides the kinetic effects related to ISC within the mechanism of sequential multiphoton absorption (Figure 1), the role of Br as peripheral substituent was not further considered in the analysis of the NLT behavior of brominated conjugated complexes as far as the excited-state absorption properties of these halogenated systems were concerned. For this reason the preparation of a system like $Br_4(tBu_2PhO)_4NcInCl$ (**1**) (Chart 1) has been accomplished, in which the four Br atoms are expected to warrant fast and efficient triplet excited-state formation due to heavy-atom effect, without provoking a drastic reduction of the excited-state lifetime.

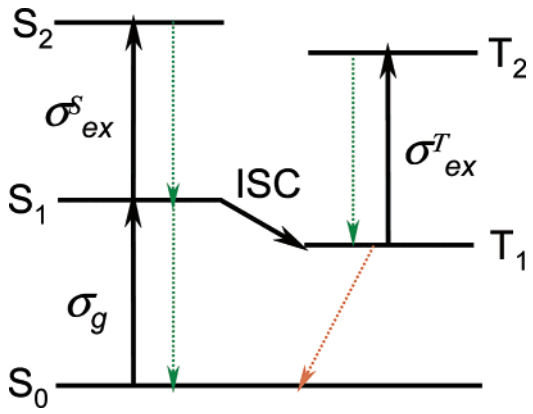

Figure 1. Jablonski diagram for the description of the mechanism of reverse saturable absorption (RSA) upon short-pulse irradiation of Pcs and analogues, in the visible spectrum. S_0, $S_{1(2)}$, and $T_{1(2)}$ indicate the ground singlet state, the first (second) excited singlet state, and the first (second) excited triplet state, respectively. The cromophore absorbs the first photon through the transition [$S_0 \rightarrow S_1$] and, depending on the dynamics of the irradiated system, will absorb sequentially a second photon through either the [$S_1 \rightarrow S_2$] or the [$T_1 \rightarrow T_2$] transition. $\sigma_{exc}^{S(T)}$ and σ_g are the absorption cross sections from the excited singlet (triplet) state and the ground state, respectively. Skewed and straight dotted arrows indicate phosphorescence and fluorescence, respectively. ISC stands for intersystem crossing [$S_1 \rightarrow T_1$]. For the sake of clarity, only the fundamental vibrational level of the various electronic levels has been indicated.

Experimental Section

1,2-Dibromo-4,5-bis(dibromomethyl)benzene (4). To 26.4 g of 1,2-dibromo-4,5-dimethylbenzene[25] (**3**, 0.1 mol) in CCl_4 (250 mL), 90 g of NBS (0.5 mol) and 0.1 g of azobis-(isobutyronitrile) (AIBN) were added. The mixture was stirred and irradiated with a UV lamp for 8 h under reflux. The mixture was hot filtered, and the remaining solid was washed with more hot CCl_4 (100 mL). The filtrate was concentrated to produce an orange yellowish solid, which was washed portionwise with 750 mL *n*-hexane and dried at 40 °C under vacuum to give 50 g of **4** (85% yield). MS (EI, 70 eV): 579.5 [M^+], 499.6 [$M^+ -$ Br] 419.7 [$M^+ - 2$ Br], 259.8 [$M^+ - 4$ Br]. For the successive synthesis of 6,7-dibromodicyanonaphthalene (**5**), the precursor **4** was used without any further purification.

6,7-Dibromodicyanonaphthalene (5). A mixture of 29 g of 1,2-di-bromo-4,5-bis(dibromomethyl)benzene (**4**) (0.05 mol), 4 g of fumaronitrile (0.06 mol), and 12 g of NaI (0.08 mol) in 200 mL of dry DMF was heated at 80 °C for 7 h and allowed to stand at room temperature for an additional 4 h. The reaction product was poured into 0.5 L of water, and then $NaHSO_3$ (8 g) was added. The resulting suspension was filtered, washed with water, and dried. The product was recrystallized from toluene−hexane mixture (1:1) to give 11 g of **5** (65% yield). MS (EI, 70 eV): 336.0 [M^+], 256.31 [$M^+ -$ Br], ^{1}H NMR (DMSO-d_6, δ): 8.72 (s, 2H, H-4), 8.86 (s, 2H, H-2), ^{13}C NMR (DMSO-d_6): 113.0 (CN), 115.4 (C-1), 121.1 (C-5), 126.0 (C-3), 130.71 (C-2), 136.1 (C-4).

6-Bromo-7-[(3,5-di-*tert*-butyl)phenoxy]-2,3-dicyanonaphthalene (6). 3.36 g. of 6,7-dibromodicyanonaphthalene (**5**)[26] (10 mmol), 2.27 g of 3,5-di-*tert*-butylphenol (11 mmol), and 9 g of K_2CO_3 (66 mmol) were mixed together in DMF (50 mL) under argon and heated at 100 °C for 3 h (the completion of the reaction was followed with thin-layer chromatography using dichloromethane as solvent). The mixture was cooled till room temperature and then stirred upon addition of 0.4 L of ice water. After 1 h of stirring the white-yellowish solid was collected and washed again with water. The compound was dried in a

vacuum at 70 °C overnight. Recrystallization from ethanol gave 4.5 g of **6** (97%). MS (EI, 70 eV): 461.3 [M^+], 435.3 [$M^+ - CN$], 381.3 [$M^+ - Br$]. ^1H NMR ($CDCl_3$, δ): 1.30 (s, 18H, $C(CH_3)_3$), 6.66 (d, 2H, H-9), 7.38 (t, 1H, H-11), 7.69 (s, 1H, H-5), 8.40 (s, 1H, H-7), 8.61 (s, 1H, H-3), 8.79 (s, 1H, H-2). ^{13}C NMR ($CDCl_3$): 29.7, 29.9 (CH_3), 35.3, (C-tBu), 106.0, 106.3 (C-1), 110.0 (CBr), 113.2 (CN), 115.4 (C-5), 116.0 (C-11), 124.7, 126.0 (C-6), 127.4 (C-7), 136.0 (C-9), 138.7 (C-3), 148.4 (C-4), 151.0 (C-8), 156.0 (C-10).

Chloro Indium(III) 2-Tetrabromo-3-tetra-(3,5-di-*tert*-butylphenyloxy)naphthalocyanine [$Br_4(tBu_2PhO)_4NcInCl$] (1). 6-Bromo-7-[(3,5-di-*tert*-butyl)phenoxy]-2,3-dicyanonaphthalene (**6**) (1.4 g, 3 mmol) and $InCl_3$ (220.0 mg, 1 mmol) were mixed in 1-chloronaphthalene (1 mL) and heated at 195 °C for 3.5 h. After the reaction mixture cooled, it was poured into methanol (100 mL) and stirred. The precipitate was collected and washed with hot methanol to give **1** as a dark yellow-green solid (0.40 g, yield: 52%). MS-FAB (*m*/*z*): 1995.1 (M^+), 1015.2 ($M^+ - Br$). ^1H NMR (THF-d_8, δ): 1.33 (s, br, 72H, CH_3), 7.06, 7.39 (br, 12H, phenoxy), 8.17, 8.28 (br, 8H on C-2), 10.81 (br, 8H on C-4). ^{13}C NMR (THF-d_8): 30.7 (CH_3), 34.9 (C-CH_3), 114.6 (br, C-8, C-10), 118.9 (br, C-2,C-4), 134.2 (br, C-3, C-5), 135.3 (br, C-6), 153.3 (br, C-7), 155.5 (br, C-1).

6,7-Di[(3,5-di-*tert*-butyl)phenoxy]-2,3-dicyanonaphthalene (7). 3.36 g of **5**[26] (10 mmol), 4.55 g of 3,5-di-*tert*-butylphenol (22 mmol), and 11 g of K_2CO_3 (80 mmol) were mixed together in DMF (60 mL) under argon and heated at 100 °C for 7 h (the completion of the reaction was followed with thin-layer chromatography using dichloromethane as solvent). The mixture was cooled till room temperature and then stirred upon addition of 0.4 L of ice water. After 1 h of stirring, the white-yellowish solid was collected and washed again with water. The compound was dried in a vacuum at 70 °C overnight. Recrystallization from ethanol gave 5.5 g of **7** (94%). MS (EI, 70 eV): 586.8 [M^+], 561.8 [$M^+ - CN$]. ^1H NMR ($CDCl_3$, δ): 1.30 (br, 36H, $C(CH_3)_3$), 6.74 (d, 4H, H-7), 7.30 (t, 2H, H-9), 7.72 (s, 2H, H-4), 8.55 (s, 2H, H-2). ^{13}C NMR ($CDCl_3$): 29.7, 29.9 (CH_3), 35.3, (C-tBu), 105.1, (C-1), 113.4 (CN), 120.0 (C-4), 121.2.0 (C-3), 124.7, (C-2), 127.4 (C-7), 138.0 (C-5), 148.7 (C-8), 153.0 (C-6).

Chloro Indium(III) 2,3-Octa-(3,5-di-*tert*-butylphenyloxy)-naphthalocyanine [$(tBu_2PhO)_8NcInCl$] (2). 6,7-Di[(3,5-di-*tert*-butyl)phenoxy]-2,3-dicyanonaphthalene (**7**) (2.35 g, 4 mmol) and $InCl_3$ (300.0 mg, 1.4 mmol) were mixed in 1-chloronaphthalene (1.5 mL) and heated to 195 °C for 3.5 h. After the reaction mixture cooled, it was poured into methanol (100 mL) and stirred. The precipitate was collected and washed with hot methanol to give **2** as a dark yellow-green solid (1.2 g, yield: 48%). MS-FD (*m*/*z*): 2497.6 (M^+). UV−Vis (nm, in toluene): 804 (λ_{max}), 742, 711, 371. ^1H NMR (THF-d_8, δ) 1.33 (s, br, 144H, CH_3), 7.03, 7.23, 7.44 (3s, 24H, phenoxy), 7.89, (s, 8H on C-2), 9.55 (br, 8H on C-4). ^{13}C NMR (THF-d_8): 30.9 (CH_3), 34.9 (C−CH_3), 113.8, 114.2 (br, C-8, C-10), 118.9, 121.7 (br, C-2,C-4), 131.3, 133.3 (br, C-3, C-5), 134.3 (br, C-6), 152.9 (br, C-7), 156.0 (br, C-1).

Apparatus for *Z*-scan Experiments. The description of the experimental setup for the nanosecond nonlinear transmission experiments with the *Z*-scan technique[27] has been previously reported by us.[2d] In the *Z*-scan experiments a doubled Nd:YAG laser was used for generating the nanosecond pulsed beam at 532 nm (pulse width: 8 ns). The experimental beam profile for *Z*-scan experiments fit a Gaussian beam profile with a correlation higher than 95%. A spatial filter transmitting only the 10% of the full beam is placed in front of the sample before focusing the input laser beam on the sample, which provides a top-hat intensity profile. The frequency of sample irradiation

SCHEME 1. Preparation of 6,7-Dibromodicyanonaphthalene (5)[a]

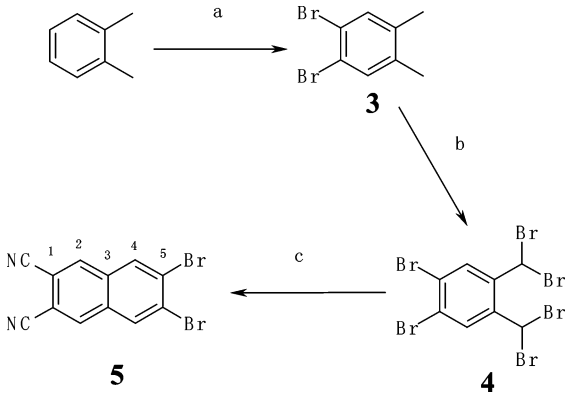

[a] Reagents and conditions: (a) Br_2, I_2, from −5 till room temperature, 16 h; (b) NBS, AIBN, UV irradiation, CCl_4 (reflux), 8 h; (c) fumaronitrile, NaI, DMF, 80 °C, 7 h.

was 10 Hz in all *Z*-scan experiments. The energy of the incident beam was varied with suitable half waveplate/polarizer combinations. f/5 focusing optics were used for excitation in all experiments whereas the optics of collection in the open aperture configuration was f/0.8. In the *Z*-scan experiments, the sample was a thin layer of a solution of **1** in deaerated toluene, which was tightly sandwiched between two CaF_2 optical windows. The CaF_2 optical windows were separated by a thin flexible polymeric membrane with rest thickness of approximately 30 μm. The cell thickness was evaluated interferometrically. The sample was translated along the beam axis and through the focal plane by means of a computer controlled translation stage. The beam radius was measured by a knife-edge technique to be 1.5 μm. In the closed-aperture configuration the measured energy corresponds to 40% of the total energy transmitted by the sample due to the insertion of a spatial filter in front of the energy detector.

Nonlinear Transmission Measurements. Deaerated solutions of **1** and **2** in toluene at different concentrations were put in quartz cuvettes with 2 mm path for the determination of nonlinear transmission measurement. The focusing optics were f/5 with the focus placed approximately at the center of the solution. The experimental setup was similar to the one described in ref 28 with the use of a doubled, Q-switched Nd:YAG laser producing 5 ns long pulses.

Results and Discussion

Synthesis of Naphthalocyanines 1 and 2. Naphthalocyanines $Br_4(tBu_2PhO)_4NcInCl$ (**1**) and $(tBu_2PhO)_8NcInCl$ (**2**) are directly obtained from the template reaction between the corresponding dinitriles (**6** and **7** for **1** and **2**, respectively) and indium thrichloride at high temperature (approximately 200 °C). The formation of dinitriles **6** and **7** requires the preparation and the isolation of 6,7-dibromodicyanonaphthalene (**5**) as precursor. The multistep procedure for the synthesis of precursor **5** starts with the bromination of *o*-xylene to give 1,2-dibromo-4,5-dimethylbenzene (**3**) (step a in Scheme 1).

Compound **3** is successively brominated with NBS on the two adjacent methyl groups under UV irradiation and in the presence of the radical generator AIBN with resulting formation of 1,2-dibromo-4,5-bis(dibromomethyl)benzene (**4**) (step b in Scheme 1). 6,7-Dibromodicyanonaphthalene (**5**) is obtained upon addition of fumaronitrile to the two aliphatic carbon atoms of **4** and the simultaneous elimination of four bromine atoms

as HBr and IBr from the dibromomethyl groups of **4** (step c in Scheme 1).

Dinitriles **6** and **7** are produced in basic conditions upon replacement of one and two bromine atoms in 6,7-dibromodicyanonaphthalene (**5**), respectively, with the 3,5-di-*tert*-butylphenoxy group generated from the deprotonation of 3,5-di-*tert*-butylphenol (Scheme 2).

SCHEME 2. Preparation of Dinitriles 6 and 7[a]

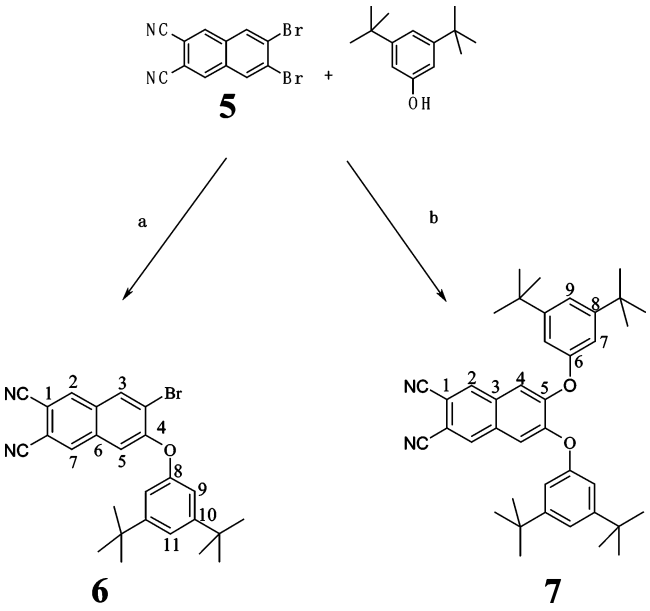

[a] Reagents and conditions: (a) 1 equiv of **5**, 1.1 equiv of 3,5-di-*tert*-butylphenol, 6 equiv of K_2CO_3, 100 °C, 4 h; (b) 1 equiv of **5**, 2.2 equiv of 3,5-di-*tert*-butylphenol, 8 equiv of K_2CO_3, 100 °C, 7 h.

Dinitriles **6** and **7** can be selectively formed under similar conditions upon variation of the number of equivalents of 3,5-di-*tert*-butylphenol with respect to a fixed amount of 6,7-dibromodicyanonaphthalene (**5**) (Scheme 2). When the molar ratio of **5** to 3,5-di-*tert*-butylphenol is one precursor **6** is preferentially formed (step a in Scheme 2). If the molar ratio of **5** to 3,5-di-*tert*-butylphenol is two the formation of precursor **7** is then favored (step b in Scheme 2).

Linear Optical Properties. The optical spectra of $Br_4(tBu_2PhO)_4NcInCl$ (**1**) in toluene at different concentration (C) values are presented in Figure 2 as variations of the molar extinction coefficient (ϵ) with the wavelength (λ).

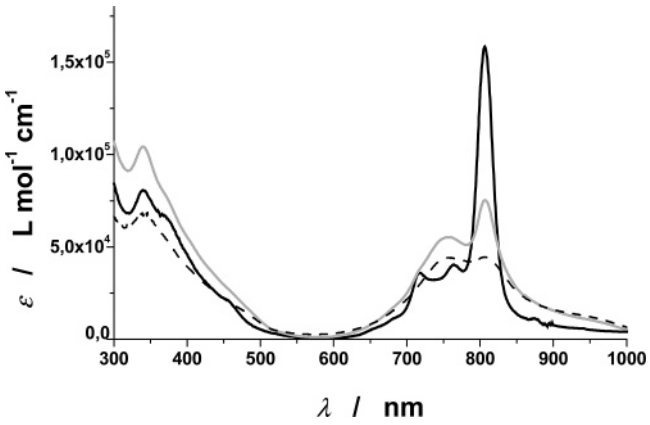

Figure 2. Variation of the molar extinction coefficient (ϵ) with the wavelength (λ) at different concentrations (C) of $Br_4(tBu_2PhO)_4NcInCl$ (**1**) in toluene. $C = 1.4 \times 10^{-5}$ M (cuvette thickness $d = 10$ mm, solid black line); $C = 7.0 \times 10^{-4}$ M (cuvette thickness $d = 0.2$ mm, solid gray line); $C = 2 \times 10^{-2}$ M ($d = 30$ μm, dashed line).

In the dilute solution complex **1** displays Q-band absorption at 806 nm with the group of vibronic satellite bands peaked at 764 and 716 nm, whereas B-band absorption is centered at 339 nm (full line spectrum in Figure 2). The largest variations of ϵ with concentration are observed at wavelengths near the Q-band for $Br_4(tBu_2PhO)_4NcInCl$ (**1**) (Figure 2). The maximum value of ϵ_{Q-band} is 1.6×10^5 L mol^{-1} cm^{-1} within the concentration range $1.4 \times 10^{-5} < C < 1.5 \times 10^{-4}$ M. When the concentration of **1** in toluene increases from 1.5×10^{-4} to 2.0×10^{-2} M ϵ_{Q-band} steadily decreases from the maximum value to 4.5×10^4 L mol^{-1} cm^{-1}. A partially resolved, broad band centered at about 760 nm (gray and dashed line spectra in Figure 2) appears when $C > 1.5 \times 10^{-4}$ M. The molar extinction coefficient for this new additional band reaches a maximum value 6×10^4 L mol^{-1} cm^{-1} when $C = 7 \times 10^{-4}$ M (gray line spectrum in Figure 2). Upon further increase of concentration of **1**, ϵ gradually decreases at 760 nm (dashed line spectrum in Figure 2).

The intensity of the 760 nm band increases at the expense of the Q-band transition. Such a spectral evolution with concentration is thought to arise from the onset of optical absorption at about 750 nm from aggregated forms of $Br_4(tBu_2PhO)_4NcInCl$ (**1**).[18a] In this context, the energy levels of $Br_4(tBu_2PhO)_4NcInCl$ aggregates can be considered as perturbed levels of **1** in the nonaggregated state.[29] From the observed changes of the absorptive properties of **1** with concentration, the aggregates are expected to be dimers or higher order oligomers with predominantly cofacial arrangement.[18b,30] In fact, exciton-coupling models account for the allowance of a transition resulting into a blue-shifted Q-band for cofacially aggregated complexes of Pcs (or Ncs).[29,31]

The occurrence of absorption in the range 800−1000 nm in the spectra of $Br_4(tBu_2PhO)_4NcInCl$ (**1**) (Figure 2) is probably associated with electronic transitions involving the partial or full exchange of charge between the naphthalocyaninato ligand and the central metal indium.[32] A relatively weak dependence on concentration was observed for the NIR absorption of **1**.

Nonlinear Optical Properties. The nonlinear optical absorption and refraction of $Br_4(tBu_2PhO)_4NcInCl$ (**1**) have been studied with the *Z*-scan technique[27] using nanosecond laser pulses at 532 nm. In *Z*-scan experiments, the transmittance (T) of the sample is measured as a function of the sample position along the optical axis. For Figure 3, the transmitted radiation is collected at the detector through an open aperture while Figure 4 represents the ratio of the light transmitted through 40% aperture divided by the light transmitted by the open-aperture experiment.

In the profiles of Figures 3 and 4, the zero position corresponds to the location of the focal plane. The sample was a thin layer (thickness, $L = 30$ μm) of a highly concentrated solution of **1** ($C = 2.0 \times 10^{-2}$ M) in toluene. Such a configuration is required since the sample thickness has to be smaller than the Rayleigh range Z_R of the Gaussian beam in *Z*-scan experiments (L and Z_R are 30 and about 50 μm, respectively). This allows the generation of uniform optical fields within the sample when this is positioned in the proximity of the focal plane of the Gaussian beam.[27,33] A highly concentrated solution of $Br_4(tBu_2PhO)_4NcInCl$ (**1**) was chosen for these experiments in order to maximize the nonlinear optical signal, which is proportional to the amount of molecular material in the sample.[2d,8c] Moreover, the decrease of the molar extinction coefficient of **1** with concentration (see Figure 2) allows the realization of an optical attenuator with relatively lower absorption in the linear optical regime as required for some applications.[3d,3e,34]

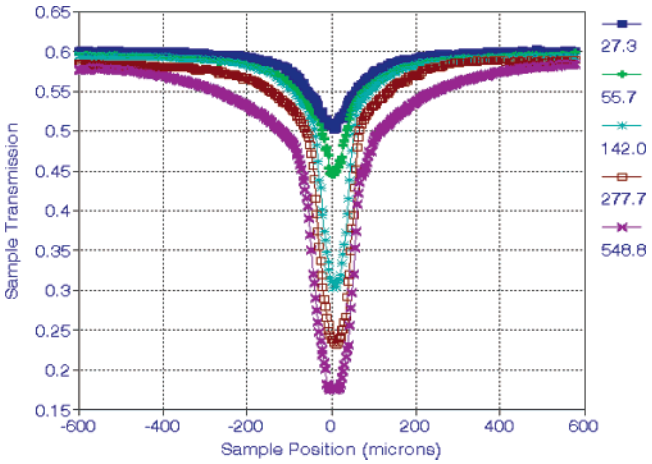

Figure 3. *Z*-scan profiles of the transmission of $Br_4(tBu_2PhO)_4NcInCl$ (**1**) in toluene at 532 nm ($C = 2 \times 10^{-2}$ M; $d = 30$ μm) in the open-aperture configuration. On *X*-axis the distance between the sample and the focus (located at $Z = 0$) is reported. The value of the incident energy is specified in nJ for each profile on the upper part of the right side.

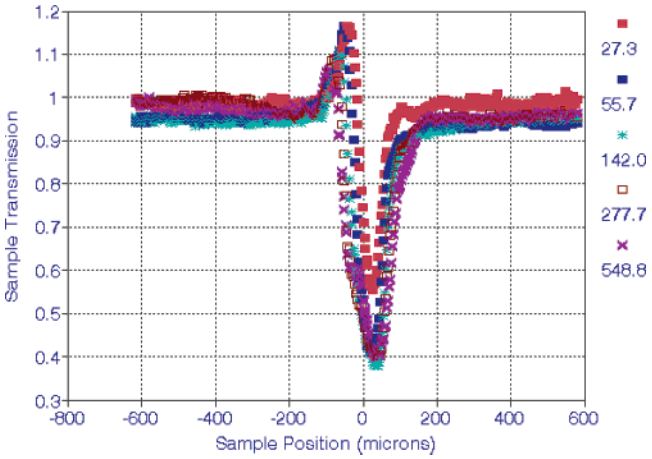

Figure 4. Normalized *Z*-scan profiles of the refractive part of the relative transmission of $Br_4(tBu_2PhO)_4NcInCl$ (**1**) in toluene at 532 nm ($C = 2 \times 10^{-2}$ M; $d = 30$ μm). Data are the ratio of the closed-aperture transmission divided by the open-aperture transmission. On the *X*-axis the distance between the sample and the focus (located at $Z = 0$) is reported. The value of the incident energy is specified in nJ for each profile on the upper part of the right side.

The linear transmittance (T_0) of the sample for nonlinear optical measurements at 532 nm was 0.61. The laser wavelength is approximately at the center of the highly transmissive window of $Br_4(tBu_2PhO)_4NcInCl$ (**1**) in which $\epsilon < 10^4$ L mol^{-1} cm^{-1}. This corresponds to the spectral region ranging from about 480 nm to 675 nm in the high concentration spectrum of **1** (dashed line in Figure 2). The wavelength of analysis (532 nm) is a standard one for the evaluation of the NLT properties of materials,[1a,b] and, in the case of Ncs, such a value does not correspond to the wavelength of their maximum nonlinear absorption (approximately 620 nm).[3a] The energy of the incident radiation (E_{in}) was varied over the range $0.2 < E_{in} < 550$ nJ. This interval corresponds to the range of peak fluence (F_{in}) $3 \times 10^{-3} < F_{in} < 10$ J cm^{-2}, which is experienced by the sample (the area of the spot at the beam focus is approximately 6×10^{-8} cm^2 being the beam waist 1.5 μm at the focus).

The *Z*-scan profiles of **1** in toluene in the open-aperture configuration are shown in Figure 3. At each of the excitation energies, the concentrated solution of tetrabrominated NcInCl **1** in toluene shows a decreasing transmission as the focal position is approached and incident fluence increases. This implies that $Br_4(tBu_2PhO)_4NcInCl$ (**1**) has a positive nonlinear absorption coefficient,[27,35] and behaves as a reverse saturable absorber for nanosecond pulses at 532 nm. These features indicate that concentrated solutions of $Br_4(tBu_2PhO)_4NcInCl$ (**1**) can act as optical attenuators[1a,1b,36] for nanosecond pulses at 532 nm.

The refractive component of the nonlinear response derived from the closed-aperture *Z*-scans profiles have been also determined for **1** (Figure 4) at the same values of incident energies that were used for the determination of the open-aperture *Z*-scans in Figure 3. Similar to what we previously observed for a side-by-side dimeric binuclear phthalocyanine[8c] $Br_4(tBu_2PhO)_4NcInCl$ (**1**) also displayed a series of unsymmetrical profiles of the *Z*-scans with respect to the focal plane at $Z = 0$ for the different values of the incident energy. This feature of the closed-aperture transmission curves does not make possible a quantitative analysis of the nonlinear refractive properties of **1** at 532 nm. However, the peak-valley shape of the closed-aperture profiles in Figure 4 demonstrates an increase of transmittance at prefocal sample positions ($Z < 0$) due to a focusing effect of the sample. When the sample traverses the path comprised between the focus and the closed aperture (i.e., for $Z > 0$), a defocusing effect is observed instead. This trend is indicative of a negative variation of the refractive index upon increase of the incident energy in the nonlinear optical regime of $Br_4(tBu_2PhO)_4NcInCl$ (**1**) in toluene solutions.[35] Such a negative contribution clearly has a thermal component, but the asymmetry of the data indicates the coexistence of an excited-state contribution also of negative sign to the nonlinear variation of the refractive index of **1**. The transmission of **1** at the focal plane as a function of incident energy E_{in} is shown in Figure 5 by plotting the minima of transmission of **1** from the open-aperture profiles of Figure 3.

The data shows that the threshold for NLT, defined as the incident energy at which the transmission is half the linear transmission, is ca. 140 nJ (in our experimental conditions this energy value corresponds to $F_{in} \approx 2.3$ J cm^{-2}) (Figure 5). This threshold is larger than that observed for Pcs, which is not surprising given that 532 nm is near the edge of the nonlinear absorption band.

For the evaluation of σ_{exc} (excited-state absorption cross section) and α_{NL} (nonlinear absorption coefficient) of $Br_4(tBu_2PhO)_4NcInCl$ (**1**) at 532 nm, it is more convenient to plot the reciprocal of the normalized nonlinear optical transmission at

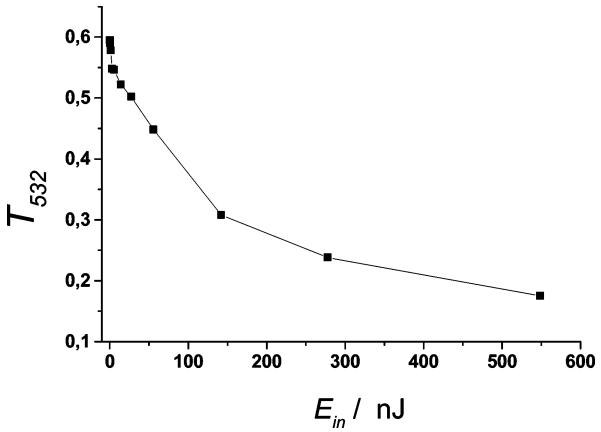

Figure 5. Variation of the nonlinear optical transmission at 532 nm for $Br_4(tBu_2PhO)_4NcInCl$ (**1**) in toluene ($C = 2 \times 10^{-2}$ M; $d = 30$ μm) when the thin-layer sample is located on the focal plane of the Gaussian beam. Points are extracted from the corrected minima of the *Z*-scan profiles determined in the open-aperture configuration.

532 nm versus incident fluence. This is because sequential two-photon absorbers such as $Br_4(tBu_2PhO)_4NcInCl$ (**1**) display a variation of transmittance through the sample which is governed by the relationship:[1a,2d,37]

$$\frac{T_0}{T} = 1 + \alpha_{NL} L_{eff} F_{in} \quad (1)$$

when the sample is an optically thin specimen. In eq 1, L_{eff} represents the effective length of the optical path (in μm), which is defined as $[1 - \exp(-\alpha_0 L)]/\alpha_0$ (α_0 and L are the linear absorption coefficient at the given wavelength and the actual length of the optical path in μm, respectively). For simple three level systems, where α_{NL} is a constant, the excited-state absorption cross section σ_{exc} can be directly determined via the equation:[1a,2d,8c,37]

$$\sigma_{exc} = \sigma_0 + \frac{2(h\nu)\alpha_{NL}}{N_T \sigma_0} \quad (2)$$

where N_T, σ_0, and $h\nu$ represent the total density of the molecular absorber (in cm^{-3}), the ground-state absorption cross section (in cm^{-2}) at the wavelength of analysis, and the energy of the single photon (in J) at the analyzed wavelength, respectively. Figure 6 shows the entire range of the reciprocal transmission as a function of excitation fluence and demonstrates that **1** is *not* well-described as a simple three-level system since the slope of the plot varies with increasing fluence. Nevertheless, analysis of the different fluence regions allows one to extract effective cross sections for the multilevel system.

Application of eq 1 gives the slope value 2 ± 0.14 cm^2 J^{-1} when only the experimental points comprised in the range $0 < F_{in} < 100$ mJ cm^{-2} are fitted (Figure 7). In this range the resulting value of the nonlinear absorption coefficient of $Br_4(tBu_2PhO)_4NcInCl$ (**1**) is $\alpha_{NL} = 844.4$ cm J^{-1} since $\alpha_0 = 156$ cm^{-1} at 532 nm, $L = 30$ μm, and $L_{eff} = 23.7$ μm in the adopted experimental conditions. For the 2×10^{-2} M solution of **1** in toluene, the linear transmittance T_0 is 0.63 at 532 nm, which corresponds to the absorbance value 0.2. From eq 2, it is found that the value of the effective excited-state absorption cross section of $Br_4(tBu_2PhO)_4NcInCl$ (**1**) at 532 nm is 1.75×10^{-17} cm^2 at the onset of the nonlinear optical behavior being $N_T = 1.2 \times 10^{19}$ cm^{-3} and $\sigma_0 = 1.3 \times 10^{-17}$ cm^2 at the photon energy $h\nu = 3.74 \times 10^{-19}$ J.

Over the incident fluence range $0.1 < F_{in} < 10$ J cm^{-2} the linear fitting of the experimental data (Figure 8) with eq 1 gives

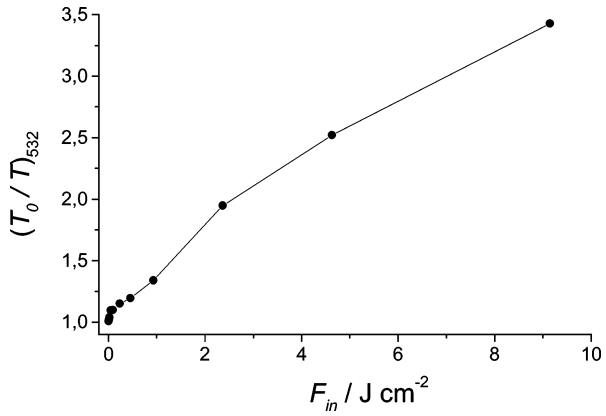

Figure 6. Variation of the reciprocal of the normalized nonlinear optical transmission at 532 nm $(T_0/T)_{532}$ for $Br_4(tBu_2PhO)_4NcInCl$ (**1**) in toluene ($C = 2 \times 10^{-2}$ M; $d = 30$ μm) as a function of the incident fluence F_{in}.

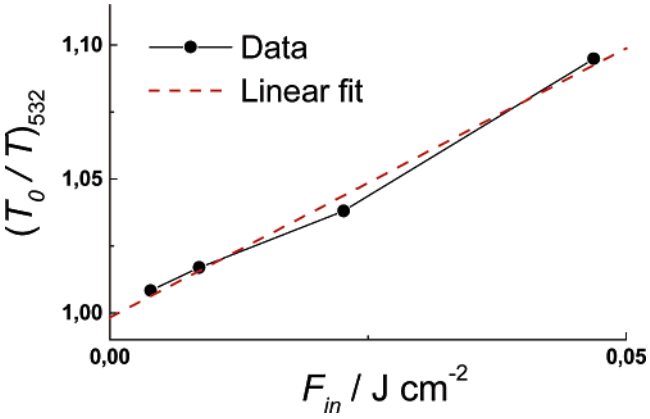

Figure 7. Variation of the reciprocal of the normalized nonlinear optical transmission at 532 nm $(T_0/T)_{532}$ for $Br_4(tBu_2PhO)_4NcInCl$ (**1**) in toluene ($C = 2 \times 10^{-2}$ M; $d = 30$ μm) and best linear fit as a function of the incident fluence F_{in} at the onset of the nonlinear optical behavior.

a slope value of 0.27 ± 0.01 cm^2 J^{-1}. The resulting value of the nonlinear absorption coefficient of $Br_4(tBu_2PhO)_4NcInCl$ (**1**) is $\alpha_{NL} = 114$ cm J^{-1} and, from eq 2, $\sigma_{exc} = 1.35 \times 10^{-17}$ cm^2 for **1** at 532 nm.

The variation of the slope of nonlinear optical transmission of the high concentrated solution of $Br_4(tBu_2PhO)_4NcInCl$ (**1**) is ascribed to the involvement of distinct excited states of **1** having different absorption properties, which are generated with increasing doses of irradiation.[38] In the present case, both excited states of $Br_4(tBu_2PhO)_4NcInCl$ (**1**) present absorption cross section values at 532 nm which are larger than the respective values in the ground state, thus giving rise to the effect of RSA at 532 nm over the whole range of incident fluence. A qualitative description of the mechanism of multiphoton absorption of $Br_4(tBu_2PhO)_4NcInCl$ (**1**) at high concentration is presented in Figure 9.

At lower incident fluences ($F_{in} < 0.1$ J cm^{-2}) the system initially absorbs a photon from the ground state with $\sigma_0 = 1.3 \times 10^{-17}$ cm^2 and, successively, a second photon from a first excited singlet or triplet state with an effective cross section, $\sigma_{exc}(1) = 1.75 \times 10^{-17}$ cm^2. At higher incident fluences ($F_{in} > 0.1$ J cm^{-2}) the system is able to pump a third excited state formed during the pulse and with a sufficiently long lifetime (longer than the pulse duration) for the further absorption of the third photon with $\sigma_{exc}(2) = 1.35 \times 10^{-17}$ cm^2 (Figure 9).

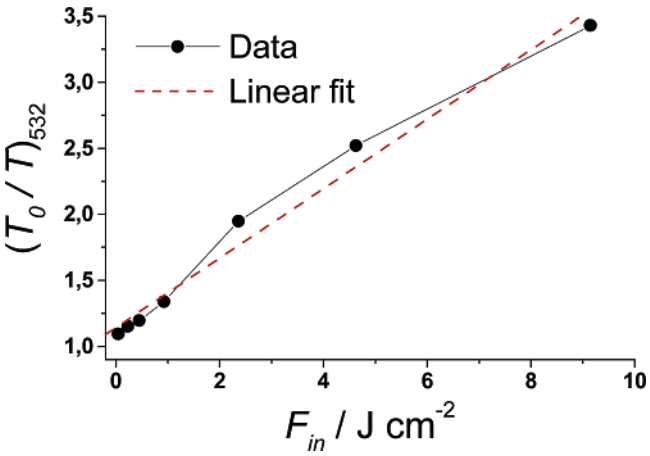

Figure 8. Variation of the reciprocal of the normalized nonlinear optical transmission at 532 nm $(T_0/T)_{532}$ for $Br_4(tBu_2PhO)_4NcInCl$ (**1**) in toluene ($C = 2 \times 10^{-2}$ M; $d = 30$ μm) and best linear fit as a function of the incident fluence in the range $0.1 < F_{in} < 10$ J cm^{-2}.

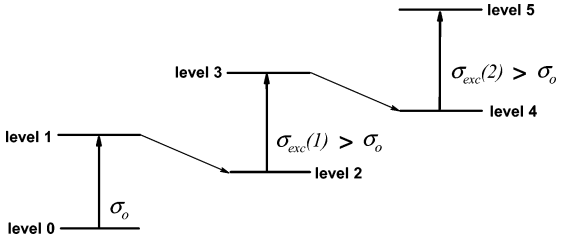

Figure 9. Qualitative description of the mechanism of multiphoton absorption in the case of high concetrated solutions of $Br_4(tBu_2PhO)_4NcInCl$ (**1**) ($C > 1 \times 10^{-3}$ M) in toluene. Decay processes and spin multiplicity for the various levels are not indicated. The symbols $\sigma_{exc}(1)$ and $\sigma_{exc}(2)$ indicate the excited-state absorption cross sections of **1** when the latter is irradiated with lower ($F_{in} < 1$ J cm^{-2}) and higher ($F_{in} > 1$ J cm^{-2}) fluence, respectively. From the fits in Figures 7 and 8, it results that $\sigma_{exc}(1) > \sigma_{exc}(2)$ and $\sigma_{exc}(1)$, $\sigma_{exc}(2) > \sigma_o$.

An evaluation of the lifetimes and the spectral properties of the distinct excited states of **1** goes beyond the scopes of the present work.

The mechanism of three-photon absorption depicted in Figure 9 operates for the nonlinear transmission effect of $Br_4(tBu_2PhO)_4NcInCl$ (**1**) at 532 nm in the whole range of concentrations of **1**. In fact, slope variations of the curves $(T_0/T)_{532}$ versus E_{in} could be found also when the nonlinear optical behavior of $Br_4(tBu_2PhO)_4NcInCl$ (**1**) was determined at different values of concentration in toluene solutions with $d = 2$ mm within the energy range $0 < E_{in} < 10$ μJ (Figure 10a). In Figure 10b, the variations of $(T_0/T)_{532}$ versus E_{in} for **1** are presented for the larger incident energy range $0 < E_{in} < 200$ μJ.

For an analysis of the variation of the nonlinear absorption properties of **1** with concentration and incident energy we have considered the linear slopes (S) of the curves in Figure 10 (Table 1).

TABLE 1: Values of the Linear Slopes $S(1)$ and $S(2)$ of the Curves in Figure 10 for 1 in the Ranges $E_{in} < E_{in}'$ and $E_{in} > E_{in}'$, Respectively[a]

C/M	$L_{eff} \times N_T\sigma_0$	$S(1)$/J^{-1}	$S(2)$/ J^{-1}	σ_{exc}*(1)/ J^{-1}	σ_{exc}*(2)/ J^{-1}	E_{in}'/μJ
0.2×10^{-3}	0.05	0.20	0.02	3.80	0.40	3.3
0.9×10^{-3}	0.35	0.55	0.13	1.60	0.37	3.1
1.3×10^{-3}	0.55	0.80	0.27	1.45	0.50	3.5
2.5×10^{-3}	0.90	1.20	0.60	1.30	0.67	3.6

[a] σ_{exc}*(n) values are obtained from the relationship: σ_{exc}*(n) = $S(n)/L_{eff}N_T\sigma_0 = S(n)/1 - T_0$. In the last column, the values of the incident energies (E_{in}') at which the slope change of the curves in Figure 10 is verified are reported.

If the parameter S is divided by L_{eff} and $N_T\sigma_0$ the resulting factor, here indicated with σ_{exc}* (Table 1), is directly proportional to the difference between the absorption cross section of the more energetic excited state of **1** involved in the multiphoton absorption process and σ_0. Therefore, in the present context σ_{exc}* might be considered as a good representation of the difference $\sigma_{exc} - \sigma_0$ [2d,5] when E_{in} replaces F_{in} in eq 1. This allows a comparative evaluation of the nonlinear transmission efficiency of the system under investigation when the sample thickness ($d = 2$ mm in the experiments of Figure 10) is larger than the Rayleigh range of the incident Gaussian beam, and the area of the beam is not constant through the sample. For the experiments of Figure 10 the beam focus was approximately located at half thickness of the sample (see Experimental Section).

Similar to the procedure adopted for the analysis of the nonlinear transmission curves of $Br_4(tBu_2PhO)_4NcInCl$ (**1**) for the thin layer sample (Figures 7 and 8), the curves in Figure 10

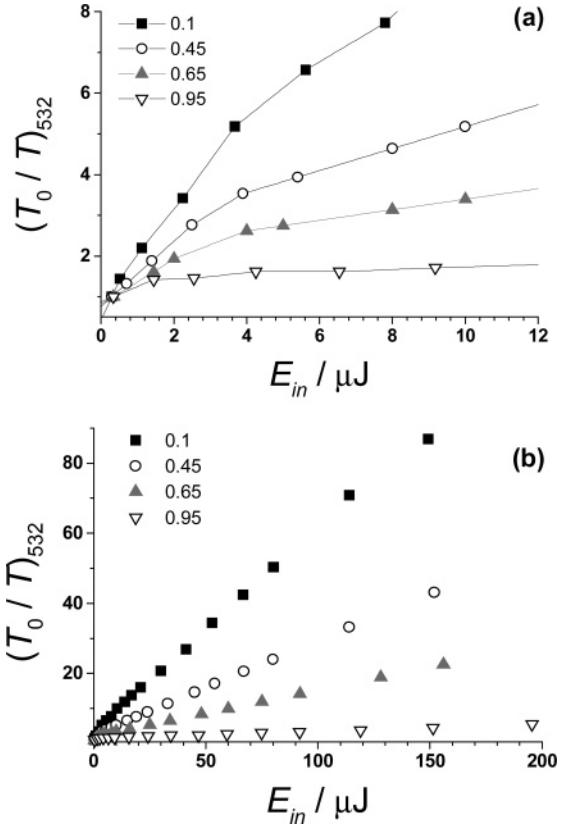

Figure 10. Variations of the inverse of the normalized optical transmission at 532 nm for $Br_4(tBu_2PhO)_4NcInCl$ (**1**) samples in toluene with different values of linear transmittance (as indicated in the legend), within small (a) and large (b) ranges of incident energy. The 2 mm thick sample is located on the focal plane of a Gaussian beam with f/5 optics of incidence. The transmitted radiation is collected through an open aperture (iris-less configuration). The corresponding concentration values for the various solutions of **1** are 2.5×10^{-3}, 1.3×10^{-3}, 0.9×10^{-3}, and 0.2×10^{-3} M in increasing order of linear transmittance.

have been also fitted with two linear trends, and the relative fitting parameters have been listed in Table 1. The linear fit for the low energy range, $E_{in} < E_{in}'$, is characterized by a general decrease of the value of σ_{exc}*(1) with increasing concentration of the photoactive material. Such a decrease of σ_{exc}*(1) could be a direct consequence of the reduction of the actual fraction of **1**, which populates the level 2 (Figure 9) due to occurrence of molecular aggregation. When the linear fit within the range $E_{in} > E_{in}'$ is considered, it is found that σ_{exc}*(2) tends to increase with C (Table 1) [σ_{exc}*(2) is related to the excited-state transition between levels 3 and 4 of **1**, Figure 9]. The direct proportionality between the values of σ_{exc}*(2) and C may imply that molecular aggregation favors the occurrence of the second excited-state transition of $Br_4(tBu_2PhO)_4NcInCl$ (**1**). Such a finding could indicate the occurrence of charge-transfer events between $Br_4(tBu_2PhO)_4NcInCl$ molecules in the excited state as a potential origin of the second transition when $E_{in} > E_{in}'$. This is because charge transfer between equal molecules would occur with higher probability at increasing molecular concentration.[39]

The curves of nonlinear transmission reported as the reciprocal of normalized transmittance vs incident energy in Figure 10 for different concentrations of $Br_4(tBu_2PhO)_4NcInCl$ (**1**) reveal that the variations of nonlinear optical transmission are dependent on the concentration of **1** when the optical path is the same for all solutions and T_0 varies accordingly.[40] It is found that the nonlinear transmission effectiveness of $Br_4(tBu_2PhO)_4NcInCl$ (**1**) increases with increasing concentration

(or decreasing linear trasmittance) when this is directly evaluated through the ratio $[(T_0 - T_{min})/T_0]$ (Table 2), T_{min} being the minimum value of transmittance reached by the system in nonlinear optical regimes without irreversible damage.[36] The analysis of the trend of the sole difference $T_0 - T_{min}$ gives the opposite trend with the concentration of $Br_4(tBu_2PhO)_4NcInCl$ (**1**) (Table 2).

TABLE 2: Values of the Various Parameters Related with the Minimum Transmittance (T_{min}) of the System for the Evaluation of the Nonlinear Transmission Effectiveness of 1 at Different Concentration Values

C/M	T_0	T_{min}	$T_0 - T_{min}$	$T_0 - T_{min}/T_0$
0.2×10^{-3}	0.95	0.180	0.77	0.812
0.9×10^{-3}	0.65	0.020	0.52	0.956
1.3×10^{-3}	0.45	0.010	0.44	0.977
2.5×10^{-3}	0.10	0.001	0.099	0.99

For sake of comparison we prepared the octasubstituted complex $(tBu_2PhO)_8NcInCl$ (**2**), which does not present any bromine atom as peripheral substituent in the structure (Chart 1). Curves of normalized nonlinear transmission for **2** in the configuration of thick film ($d = 2$ mm) have been also determined when it had different values of concentration in toluene solutions (Figure 11).

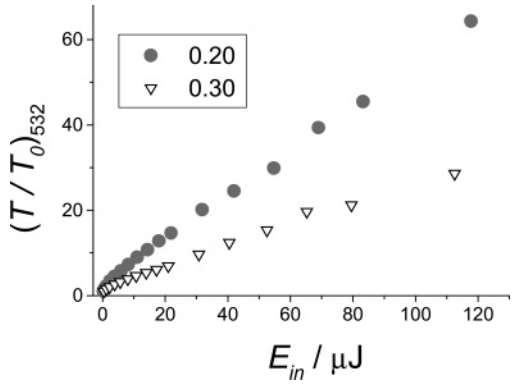

Figure 11. Variation of the inverse of the normalized optical transmission at 532 nm for $(tBu_2PhO)_8NcInCl$ (**2**) samples in toluene with different values of linear transmittance as indicated in the panel. The 2 mm thick sample is located on the focal plane of a Gaussian beam with f/5 optics of incidence. The transmitted radiation is collected through an open aperture (iris-less configuration). The corresponding concentration values for the various solutions of **2** are 4.0×10^{-3} and 2.0×10^{-3} M in increasing order of linear transmittance.

Similar to the tetrabrominated complex **1** (Figure 10), the octaphenoxy substituted system **2** presents variations of nonlinear transmission versus incident energy, which can be considered as a succession of two linear fits. The analysis of the linear fits of the two curves in Figure 11 has led to the determination of the various fitting parameters reported in Table 3.

TABLE 3: Values of the Linear Slopes *S*(1) and *S*(2) of the Curves in Figure 11 for 2 in the ranges $E_{in} < E_{in}'$ and $E_{in} > E_{in}'$, Respectively[a]

C/M	$L_{eff} \times N_T\sigma_0$	$S(1)/J^{-1}$	$S(2)/J^{-1}$	$\sigma_{exc}^*(1)/J^{-1}$	$\sigma_{exc}^*(2)/J^{-1}$	$E_{in}'/\mu J$
0.2×10^{-3}	0.70	0.61	0.24	0.87	0.34	2.4
4.0×10^{-3}	0.80	1.1	0.52	1.38	0.65	3.6

[a] $\sigma_{exc}^*(n)$ values are obtained from the relationship: $\sigma_{exc}^*(n) = S(n)/L_{eff}N_T\sigma_0 = S(n)/1 - T_0$. In the last column, the values of the incident energies E_{in}' at which the slope change of the curves in Figure 11 occurs are reported.

The value of $\sigma_{exc}^*(1)$ is generally lower for $(tBu_2PhO)_8NcInCl$ (**2**) with respect to $Br_4(tBu_2PhO)_4NcInCl$ (**1**) (Table 1), whereas $\sigma_{exc}^*(2)$ values are similar for the two chloro-indium complexes **1** and **2**. Since $\sigma_{exc}^*(1)$ as well as $\sigma_{exc}^*(2)$ represent a time-averaged value of excited-state absorption cross section, the lowest value found in the case of $(tBu_2PhO)_8NcInCl$ (**2**) can be also a consequence of the lower quantum yield of formation (Φ_{T1}) of the first triplet excited state (level 2 in Figure 9), in comparison to the brominated complex **1,** which is expected to produce a larger value of Φ_{T1} for the presence of an heavy atom like Br.[23] The variation of $\sigma_{exc}^*(1)$ with *C* is less pronounced for complex **2** with respect to **1**. This is ascribed to the weaker tendency of $(tBu_2PhO)_8NcInCl$ (**2**) with respect to $Br_4(tBu_2PhO)_4NcInCl$ (**1**) to form aggregates since a larger number of aryloxy substituents acting as molecular spacers is present in the formula of **2** (Chart 1). In contrast to tetrabrominated **1**, the octasubstituted complex $(tBu_2PhO)_8NcInCl$ (**2**) does not display a decrease of $\sigma_{exc}^*(1)$ with the increase of *C* (Table 3). Since molecular aggregation is expected to influence at a lower extent the photophysical behavior of **2** with respect to **1**, the small increase of $\sigma_{exc}^*(1)$ with *C* could be due to the lower percentage of degraded material in the more concentrated solution of **2**, which is obtained upon photoinitiated reaction of **2** with the nearly constant concentration of dissolved oxygen in toluene.

The variation of the nonlinear optical transmission of two solutions of the tetrabrominated complex **1** and $(tBu_2PhO)_8NcInCl$ (**2**) having the same linear optical density at 532 nm has been measured and compared (Figure 12).

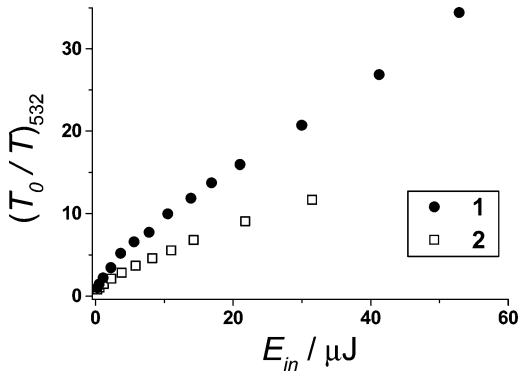

Figure 12. Variations of $(T_0/T)_{532}$ for the THF solutions of $Br_4(tBu_2PhO)_4NcInCl$ (**1**) and $(tBu_2PhO)_8NcInCl$ (**2**) with the same value of T_0 ($= 0.10$) at 532 nm. Sample thickness and optical setup are the same as in Figure 10. Concentration values are 1.6×10^{-3} and 1.8×10^{-3} M for the toluene solutions of **1** and **2**, respectively.

The latter condition of equal linear optical densities warrants the meaningfulness of the comparison between the nonlinear transmission properties of different systems since the nonlinear transmission effectiveness at a fixed wavelength is evaluated by means of the difference $(T_0 - T_{min})$ or the ratio $[(T_0 - T_{min})/T_0]$ (Table 4).[36]

TABLE 4: Values of the Various Parameters Related with the Comparative Evaluation of the Nonlinear Transmission Effectiveness of 1 and 2 Having Same Linear Transmittance ($T_0 = 0.10$) in Toluene

compd	*C*/M	T_{min}	$T_0 - T_{min}$	$T_0 - T_{min}/T_0$	DR[a]/10^{-6} J
1	1.6×10^{-3}	0.0011	0.0988	0.988	150
2	1.8×10^{-3}	0.0085	0.0915	0.915	30

[a] DR, dynamic range.

From the data of Figure 12 the nonbrominated system **2** presents a considerably smaller variation of the inverse of the

normalized transmittance at 532 nm when compared to the tetrabrominated complex **1**. This is equivalent to saying that the nonlinear transmission effect produced by $Br_4(tBu_2PhO)_4NcInCl$ (**1**) is stronger than that observed with $(tBu_2PhO)_8NcInCl$ (**2**). Moreover, the tetrabrominated system **1** shows a considerably wider dynamic range with respect to **2**, as shown by the observation of reversible changes of transmittance for **1** with incident energy values as high as 150 μJ, whereas for nonbrominated **2** the transmittance reversibly varies with only to a maximum value of 30 μJ under the same experimental conditions. The differences in dynamic ranges of $Br_4(tBu_2PhO)_4NcInCl$ (**1**) and $(tBu_2PhO)_8NcInCl$ (**2**) are associated to the higher photostability of **1**, which is induced by the presence of electronegative atoms such as Br similar to what is found in the case of fluorinated complexes.[3d,3e,14a]

Conclusions

The soluble peripherally substituted naphthalocyanineschloro indium(III) 2-tetrabromo-3-tetra-(3,5-di-*tert*-butylphenyloxy)-naphthalocyanine [$Br_4(tBu_2PhO)_4NcInCl$,**1**] and chloro indium-(III) 2,3-octa-(3,5-di-*tert*-butylphenyloxy)naphthalocyanine [$(tBu_2PhO)_8NcInCl$, **2**] have been synthesized, and their nonlinear transmission properties at 532 nm for ns laser pulses have been evaluated and analyzed. A variable slope trend for the nonlinear optical transmission of both systems with low values of fluence of the incident radiation has been found. Such a behavior has been modeled through the modification of a simpler model taking into account additional excited-state transitions that take place at higher light intensities. These additional transitions were associated to the possible occurrence of a charge transfer process between excited molecules. Partial bromination of a naphthalocyaninato chloro-indium complex in the peripheral positions of the macrocycle leads to the general improvement of the nonlinear transmission properties of such a system in comparison to a nonhalogenated chloro-indium naphthalocyanine when high fluence radiations are produced by nanosecond laser pulses at 532 nm. The observed changes in the nonlinear transmission effect generated by the two differently substituted systems, $Br_4(tBu_2PhO)_4NcInCl$ (**1**) and $(tBu_2PhO)_8NcInCl$ (**2**), are ascribed to the modification of several concomitant factors and properties like:

(i) the ground-state absorption cross sections with consequent use of different concentrations for the attainment of equal linear transmission;

(ii) the quantum yield of formation of the absorbing excited state;

(iii) the stability of the photoactive molecule in the conditions of irradiation

which all might intervene to some extent. The differences between the nonlinear optical behavior of tetrabrominated and nonhalogenated Ncs have to be ascribed also to other factors, the influence of which has not been directly evaluated in the present work. These factors include the profile of the excited-state spectrum, the transition dipole moments involved in the transitions between excited states, and the lifetime of the absorbing excited state.

The main reasons for the improved nonlinear properties of the brominated system **1** are found in the higher photostability (compare Figure 12) imparted by the presence of electronegative Br, higher yield of excited-state formation due to heavy-atom effect. Larger variations of the transition dipole moments associated with the excited-state transitions of the tetrabrominated naphthalocyaninato complex when compared to nonhalogenated system are also expected.

Acknowledgment. Financial support from EU (Contracts HPRN-CT-2000-00020 and HPRN-CT-2002-00323) is gratefully acknowledged.

References and Notes

(1) (a) Tutt, L. W.; Boggess, T. F. *Prog. Quantum Electron.* **1993**, *17*, 299−338. (b) Sun, Y. P.; Riggs, J. E. *Int. Rev. Phys. Chem.* **1999**, *18*, 43−90. (c) Xia, T.; Hagan, D. J.; Dogariu, A.; Said, A. A.; Van Stryland, E. W. *Appl. Opt.* **1997**, *36*, 4110−4122. (d) Swalen, J. D.; Kajzar, F. *Nonlinear Opt.* **2001**, *27*, 13−32. (e) Dini, D.; Barthel, M.; Hanack, M. *Eur. J. Org. Chem.* **2001**, 3759−3769.

(2) (a) Shirk, J. S.; Pong, R. G. S.; Bartoli, F. J.; Snow, A. R. *Appl. Phys. Lett.* **1993**, *63*, 1880−1882. (b) Hanack, M.; Schneider, T.; Barthel, M.; Shirk, J. S.; Flom, S. R.; Pong, R. G. S. *Coord. Chem. Rev.* **2001**, *219*−*221*, 235−258. (c) Perry, J. W.; Mansour, K.; Lee, I. Y. S.; Wu. X. L.; Bedworth, P. V.; Chen, C. T.; Ng, D.; Marder, S. R.; Miles, P.; Wada, T.; Tian, M.; Sasabe, H. *Science* **1996**, *273*, 1533−1536. (d) Shirk, J. S.; Pong, R. G. S.; Flom, S. R.; Heckmann, H.; Hanack, M. *J. Phys. Chem. A* **2000**, *104*, 1438−1449.

(3) (a) Shirk, J. S.; Flom, S. R.; Lindle, J. R.; Bartoli, F. J.; Snow, A. W.; Boyle, M. E. *Mater. Res. Soc. Symp. Proc.* **1994**, *328*, 661−666. (b) Perry, J. S.; Mansour, K.; Marder, S. R.; Chen, C. T.; Miles, P.; Kenney, M. E.; Kwag, G. *Mater. Res. Soc. Symp. Proc.* **1995**, *374*, 257−265. (c) Perry, J. S.; Mansour, K.; Miles, P.; Chen, C. T.; Marder, S. R.; Kwag, G.; Kenney, M. *Polym. Mater. Sci. Eng.* **1995**, *72*, 222−223. (d) Yang, G. Y.; Hanack, M.; Lee, Y. W.; Dini, D.; Pan, J. F. *Adv. Mater.* **2005**, *17*, 875−879. (e) Yang, G. Y.; Hanack, M.; Lee, Y. W.; Chen, Y.; Lee, M. K. Y.; Dini, D. *Chem. Eur. J.* **2003**, *9*, 2758−2762.

(4) (a) Giuliano, C. R.; Hess, L. D. *IEEE J. Quantum Electron.* **1967**, *QE-3*, 358−367. (b) Blau, W.; Byrne, H.; Dennis, W. M.; Kelly, J. M. *Opt. Commun*. **1985**, *56*, 25−29. (c) Hercher, M. *Appl. Opt.* **1967**, *6*, 947−954.

(5) Nalwa, H. S.; Shirk, J. S. In *Phthalocyanines: Properties and Applications*; Leznoff, C. C., Lever, A. B. P., Eds.; VCH: New York, 1996; Vol. 4, pp 83−181.

(6) (a) Gouterman, M.; Wagniere, G.; Snyder, L. C. *J. Mol. Spectrosc.* **1963**, *11*, 108−127. (b) Eastwood, D.; Edwards, L.; Gouterman, M.; Steinfeld, J. I. *J. Mol. Spectrosc.* **1966**, *20*, 381−390. (c) Bajema, L.; Gouterman, M.; Meyer, B. *J. Mol. Spectrosc.* **1968**, *27*, 225−235.

(7) Dini, D.; Barthel, M.; Schneider, T.; Ottmar, M.; Verma, S.; Hanack, M. *Solid State Ionics* **2003**, *165*, 289−303.

(8) (a) De la Torre, G.; Vazquez, P.; Agullo-Lopez, F.; Torres, T. *Chem. Rev.* **2004**, *104*, 3723−3750. (b) O'Flaherty, S. M.; Hold, S. V.; Cook, M. J.; Torres, T.; Chen, Y.; Hanack, M.; Blau, W. J. *Adv. Mater.* **2003**, 15, 19−32. (c) Calvete, M. J. F.; Dini, D.; Flom, S. R.; Hanack, M.; Pong, R. G. S.; Shirk, J. S. *Eur. J. Org. Chem.* **2005**, 3499−3509.

(9) (a) Hanack, M.; Heckmann, H.; Polley, R. In *Methoden der Organischen Chemie (Houben-Weyl*), 4th ed.; Thieme Verlag: Stuttgart, 1997; Vol. E9d, pp 717−842. (b) Schmid, M.; Sommerauer, M.; Geyer, M.; Hanack, M. In *Phthalocyanines: Properties and Applications*; Leznoff, C. C., Lever, A. B. P., Eds.; VCH: New York, 1996; Vol. 4, pp 5−18.

(10) (a) Schlettwein, D.; Hesse, K.; Gruhn, N. E.; Lee, P. A.; Nebesny, K. W.; Armstrong, N. R. *J. Phys. Chem. B* **2001**, *105*, 4791−4800. (b) Ghosh, A.; Gassman, P. G.; Almloef, J. *J. Am. Chem. Soc.* **1994**, *116*, 1932−1940.

(11) (a) Handa, M.; Suzuki, A.; Shoji, S.; Kasuga, K.; Sogabe, K. *Inorg. Chim. Acta* **1995**, *230*, 41−44. (b) Golovin, M. N.; Seymour, P.; Jayaraj, K.; Fu, Y. S.; Lever, A. B. P. *Inorg. Chem.* **1990**, *29*, 1719−1727. (c) D'Souza, F.; Hsieh, Y. Y.; Deviprasad, G. R. *J. Porphyrins Phthalocyanines* **1998**, *2*, 429−437. (d) Do Nascimento, E.; De Silva, G.; Caetano, F. A.; Fernandes, M. A. M.; Da Silva, D. C.; De Carvalho, M. E. M. D.; Pernaut, J. M.; Reboucas, J. S.; Idemori, Y. M. *J. Inorg. Biochem.* **2005**, *99*, 1193−1204.

(12) Yamaguchi, Y. *J. Chem. Phys.* **2005**, *122*, 184702/1−11.

(13) (a) Schollhorn, B.; Germain, J. P.; Pauly, A.; Maleysson, C.; Blanc, J. P. *Thin Solid Films* **1998**, *326*, 245−250. (b) Peisert, H.; Knupfer, M.; Zhang, F.; Petr, A.; Dunsch, L.; Fink, J. *Surf. Sci.* **2004**, *566*−*568*, 554−559. (c) Peisert, H.; Knupfer, M.; Schwieger, T.; Fuentes, G. G.; Olligs, D.; Fink, J.; Schmidt, T. *J. Appl. Phys.* **2003**, *93*, 9683−9692. (d) Oekermann, T.; Schlettwein, D.; Jaeger, N. I.; Wohrle, D. *J. Porphyrins Phthalocyanines* **1999**, *3*, 444−452.

(14) (a) Dini, D.; Yang, G. Y.; Hanack, M. *J. Chem. Phys.* **2003**, *119*, 4857−4864. (b) Dini, D.; Hanack, M.; Ji, W.; Chen, W. *Mol. Cryst. Liq. Cryst.* **2005**, *431*, 559−574. (c) Venanzi, M.; Tagliatesta, P.; Pastorini, A.; Mari, P.; Elisei, F.; Latterini, L.; Kadish, K. M. *J. Porphyrins Phthalocyanines* **2002**, *6*, 643−652.

(15) Weitman H.; Schatz S.; Gottlieb H. E.; Kobayashi N.; Ehrenberg B. *Photochem. Photobiol.* **2001**, *73*, 473−481.

(16) Cheng, W. D.; Wu, D. S.; Zhang, H.; Chen, J. T. *Phys. Rev. B* **2001**, *64*, 125109/1−11.

(17) Fuchs, H.; Zimmermann, J.; Röder, B. *Opt. Commun.* **2003**, *220*, 119−127.

(18) (a) Snow, A. W.; Jarvis, N. L. *J. Am. Chem. Soc.* **1984**, *106*, 4706−4711. (b) Snow, A. W. In *The Porphyrin Handbook*, Vol. 17; Kadish, K. M., Smith, K. M., Guilard, R., Eds.; Elsevier Science: Amsterdam, 2003; pp 129−176.

(19) Flom, S. R.; Shirk, J. S.; Pong, R. G. S.; Bartoli, F. J.; Snow, A. W.; Boyle, M. E. *Book of Abstracts*, 212th ACS National Meeting, Orlando, FL, August 25−29, 1996; PMSE−124.

(20) Ye, H.; Chang, Q.; Wu, Y.; He, C.; Zuo, X.; Zhan, J.; Wang, Y.; Song, Y. *Mater. Lett.* **2003**, *57*, 3302−3304.

(21) Song, Y.; Wang, Y.; Li, J.; Fang, G.; Yang, X.; Wu, Y.; Liu, Y.; Zuo, X.; Zhu, Q.; Chen, N. *SPIE Proc.* **1998**, *3554*, 241−245.

(22) (a) Su, W.; Cooper, T. M.; Brant, M. C. *Chem. Mater.* **1998**, *10*, 1212−1213. (b) Bonnett, R.; Harriman, A.; Kozyrev, A. N. *J. Chem. Soc., Faraday Trans.* **1992**, *88*, 763−769.

(23) Turro, N. J. *Modern Molecular Photochemistry*; University Science Books: Sausalito, CA, 1991; p 124.

(24) McEwan, K. J.; Fleitz, P. A.; Rogers, J. E.; Slagle, J. E.; McLean, D. G.; Akdas, H.; Katterle, M.; Blake, I. M.; Anderson, H. L. *Adv. Mater.* **2004**, *16*, 1933−1935.

(25) Crossley, A. W.; Smith, S. *J. Chem. Soc.* **1913**, *103*, 990−998.

(26) Kovshev, E. I.; Puchnova, V. A.; Luk'yanets, E. A. *J. Org. Chem USSR (Engl. Trans.)* **1971**, *7*, 364−366.

(27) Sheik-Bahae, M.; Said, A. A.; Wei, T. H.; Hagan, D. J.; Van Stryland, E. W. *IEEE J. Quantum Electron.* **1990**, *26*, 760−769.

(28) (a) James, D. B.; McEwan, K. J. *Mol. Cryst. Liq. Cryst., Sect. B* **1999**, *21*, 377−389; (b) Desroches, C.; Parola, S.; Vocanson, F.; Ehlinger, N.; Miele, P.; Lamartine, R.; Bouix, J.; Eriksson, A.; Lindgren, M.; Lopes, C. *J. Mater. Chem.* **2001**, *11*, 3014−3017.

(29) McKeown, N. B. *Phthalocyanine Materials*; Cambridge University Press: Cambridge, UK, 1998; pp 91−94.

(30) (a) Schutte, W. J.; Sluyters-Rehbach, M.; Sluyters, J. H. *J. Phys. Chem.* **1993**, *97*, 6069−6073. (b) Yang, Y. C.; Ward, J. R.; Seiders, R. P. *Inorg. Chem.* **1985**, *24*, 1765−1769. (c) Fuijiki, M.; Tabei, H.; Kurihara, T. *J. Phys. Chem.* **1988**, *92*, 1281−1285.

(31) Hollebone, B. R.; Stillman, M. J. *Chem. Phys. Lett.* **1974**, *29*, 284−286.

(32) Lever, A. B. P.; Pickens, S. R.; Minor, P. C.; Licoccia, S.; Ramaswamy, B. S.; Magnell, K. *J. Am. Chem. Soc.* **1981**, *103*, 6800−6806.

(33) Fischer, R. E.; Tadic-Galeb, B. *Optical System Design*; SPIE Press: McGraw-Hill: New York, 2000.

(34) Snow, A. W.; Shirk, J. S.; Bartoli, F. J., Jr.; Lindle, J. R.; Boyle, M. E.; Pong, R. G. S.; Flom, S. R.; Pinto, J. F. U.S. Patent 1998, US 5805326 A 19980908 Application: US 94-239068 19940506.

(35) Gubler, U.; Bosshard, C. In *Polymers for Photonics Applications I*; Lee, K. S., Ed.; Advances in Polymer Science Series 158; Springer-Verlag: Berlin, 2002; pp 123−191.

(36) Perry, J. W. In *Nonlinear Optics of Organic Molecules and Polymers*; Nalwa, H. S., Miyata, S., Eds.; CRC Press: Boca Raton, FL, 1997; pp 813−840.

(37) Van Stryland, E. W.; Sheik-Bahae, M.; Said, A. A.; Hagan, D. J. *Prog. Cryst. Growth Charact. Mater.* **1993**, *27*, 279−311.

(38) (a) Giuliano, C. R.; Hess, L. D. *Appl. Phys. Lett.* **1968**, *12*, 292−294. (b) Dini, D.; Vagin, S.; Hanack, M.; Amendola, V.; Meneghetti, M. *Chem. Commun.* **2005**, 3796−3798.

(39) L'Her, M.; Pondaven, A. In *The Porphyrin Handbook*, Vol. 16; Kadish, K. M., Smith, K. M., Guilard, R., Eds.; Elsevier Science: Amsterdam, 2003; pp 117−169.

(40) Riggs, J. E.; Martin, R. B.; Walker, D. B.; Guo, Z.; Sun, Y. P. *Phys. Chem. Chem. Phys.* **2004**, *6*, 703−709.